ChemComm

Accepted Manuscript

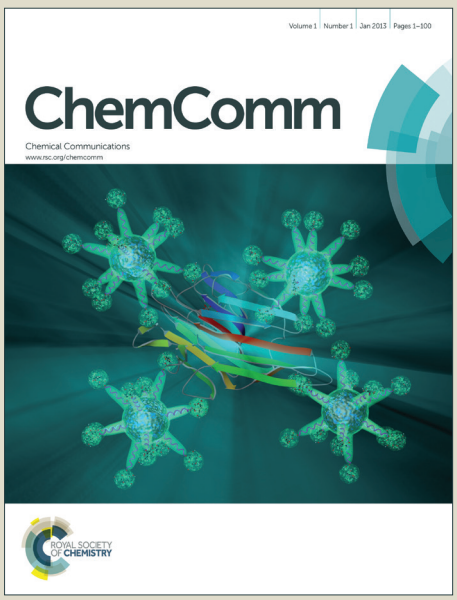

ROYAL SOCIETY OF CHEMISTRY

www.rsc.org/chemcomm

Journal Name

RSCPublishing

COMMUNICATION

H^+–Assisted Fluorescent Differentiation of Cu^+ and Cu^{2+}: Effect of Al^{3+}–induced acidity on chemical sensing and generation of two novel and independent logic gating pathways

Cite this: DOI: 10.1039/xoxxoooooox

Received ooth January 2012,
Accepted ooth January 2012

DOI: 10.1039/xoxxoooooox

www.rsc.org/

Yonghwang Ha[a], Dhiraj P. Murale[a], Changsuk Yun[a], Sudesh T. Manjare[a,b], Hyungjun Kim[a], Juhyoun Kwak[a], Yoon Sup Lee[a], David G. Churchill[a,*]

A novel Schiff base probe exhibited strong 'turn–ON' fluorescence for Cu^{2+} at 345 nm, Al^{3+} at 445 nm, and Cu^+ at 360 nm in the presence of Al^{3+} in organic solvent (acetonitrile), which allowed for construction of molecular logic gates 'INH' and '1:2 DEMULTIPLEXING.' H^+ generated from Al^{3+} highly contributed to Cu^+ chemosensing based on a redox non-innocence mechanism.

Preparation of novel synthetic systems to exploit the behavior of $Cu^{+/2+}$, especially in terms of photophysical changes, has become a very important issue for the diagnosis of disease progression. One of the best strategies for probing metal ions is fluorescence chemosensing; the sensitivity, selectivity and ease of operation are all possible. In particular, however, the differentiation by fluorescence of Cu^+ and Cu^{2+} is challenging.[1] Moreover, Cu^{2+} often imparts a quenching effect on molecular fluorescence because of its paramagnetic ability. Also, $Cu^+_{(aq)}$ can be degraded via disproportionation into Cu^0 and $Cu^{2+}_{(aq)}$. Certain chemical probes have been developed for the detection of Cu^+ [1-5] and Cu^{2+} by fluorescent "*Turn–ON*" sensing.[6-10] Some strategies in these studies for Cu^+ sensing have involved the adaptation of NS_3[2, 5] or NS_4[3] coordination environments (cyclic or acyclic thioaza groups which include nitrogen and sulfur donor atoms) or reaction–based sensing.[4] For the probing of Cu^{2+}, chelation strategy using species that include Schiff bases [6-8, 10] or reaction–based probing[9] have been used.

Meanwhile, aluminum (Al^{3+}) is an important analyte in that it can leach into the environment and induce various toxic effects on human health. *i.e.*, numerous claims have been made in the past literature involving how Al^{3+} could be linked to neurodegenerative disease incidence such as Alzheimer's disease.[11] In fact, the hydronium ion can be generated when Al^{3+} is dissolved in water. Unwanted effects of the hydronium ion as a by–product of Al^{3+} aqueous solvation [12-15] on chemical sensing has been little discussed. Nitrogen atoms in secondary or tertiary amine groups of molecular probes can provide binding sites for protonation during chemical sensing. H^+, attached to *e.g.*, amine/imine groups, can influence e.g., the photoinduced electron transfer (PET) mechanism of a probe molecule which usually decreases fluorescence intensity.[1, 16, 17] Therefore, H^+, induced by Al^{3+}, can be considered in molecular fluorescence probe design.

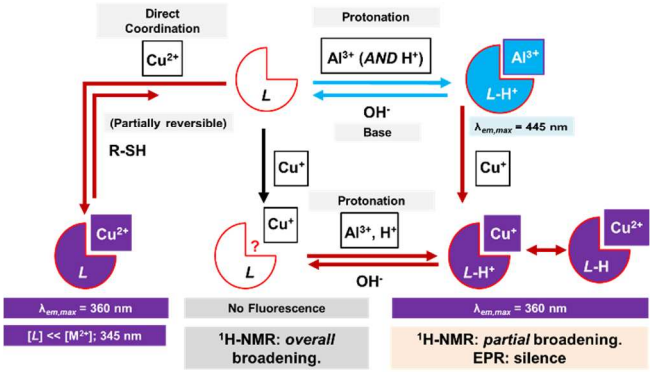

Scheme 1. Fluorescence "turn-ON" probing for Cu^+, Cu^{2+}, and Al^{3+} with Comp. **2**.

Herein, a selective probe for Al^{3+}, Cu^+ and Cu^{2+} via chelation–enhanced fluorescence (Scheme 1), involves the salicylaldamine with an *N*–dimethyl carbamoyl group, a straight–forward and simple protection of the phenol group which has been unexplored in chemosensing (Scheme 2).[18, 19] Analytical measurements were undertaken to elucidate sensitivity, selectivity, reversibility, binding analysis using fluorescence, UV-vis absorbance, ^{1}H-NMR, and EPR analysis.

When 16 kinds of metal ions were screened with fluorescence, strong fluorescence '*OFF – ON*' signals were found for two metal ions in entirely separate regions of the spectrum: for Cu^{2+} at $\lambda_{em–max}$ = 352 nm (85–*fold*), and Al^{3+} at $\lambda_{em–max}$ = 445 nm (771–*fold*), relative to the starting intensity of **2** (Figure 1(a)). These two 'turn–ON' signals in different wavelength zones allow for very minimal spectral overlap with each other, implying this probe can analyze either Cu^{2+} or Al^{3+} ions, or potentially both by fluorescence in solution.

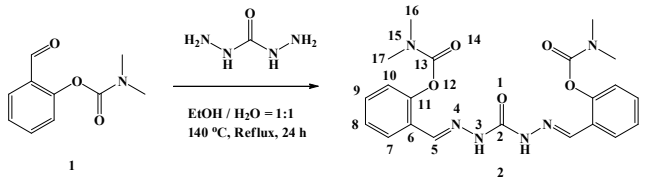

Scheme 2. Synthesis of the fluorescence probe (Comp. **2**).

Interestingly, Cu^{+} displayed a new emission intensity of 360 nm (32–*fold*), similar to Cu^{2+} (low concentration) (Figure 1(b) in the presence of Al^{3+}, whereas Cu^{+} itself did not show an emission signal. It is important to verify the influence of H^{+} generated by Al^{3+} on Cu^{+}–induced fluorescence in the presence of Al^{3+}. As shown in ESI, Figure S11, while only a small fluorescence increase was shown at ~445 nm in the presence of H^{+} only, co–incubation of Cu^{+} (10 equiv) and H^{+} (10 equiv) displayed strong fluorescence at the same wavelength of Al^{3+} and Cu^{+} co–treated solution, which strongly suggest H^{+}, generated by Al^{3+}, takes an important role for Cu^{+} fluorescence "*turn-ON*".

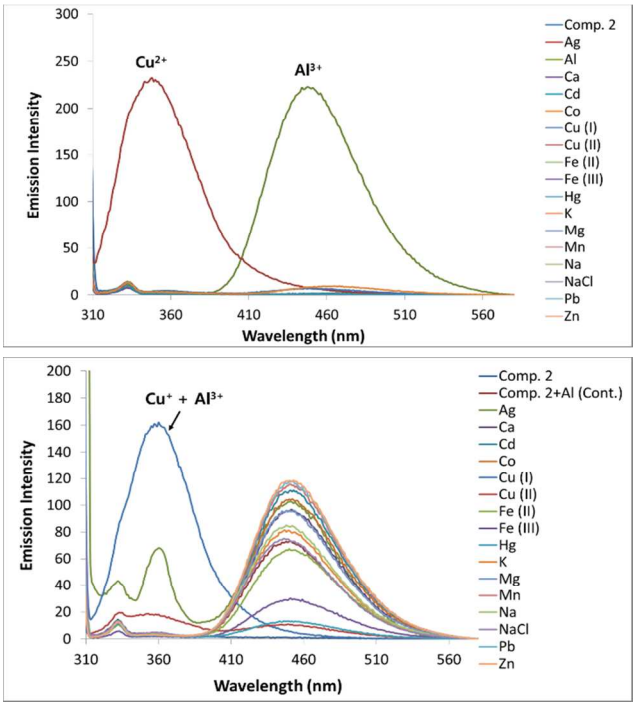

Figure 1. Emission spectrum of Comp. **2** (10 μM, 1 equiv) with Ag^{+}, Al^{3+}, Ca^{2+}, Cd^{2+}, Co^{2+}, Cu^{+}, Cu^{2+}, Fe^{2+}, Fe^{3+}, Hg^{2+}, K^{+}, Mg^{2+}, Mn^{2+}, Na^{+}, Pb^{2+}, Zn^{2+} ions (100 μM, 10 equiv). (b) Interference experiments of Comp. **2** with Al^{3+} against other metal ions. λ_{ex} = 300 nm, Slit width (EM: 5 nm, EX: 5 nm). Solvent: acetonitrile.

In accord with copper Fenton–type chemistry between Cu^{2+} and Cu^{+}, spin multiplicity was investigated for Cu^{+}, Cu^{2+} and Al^{3+} in relationship with **2** by EPR spectroscopic analysis. In Figure 2, Cu^{2+} showed a characteristic EPR spectroscopic signal.[20] Comp. **2** with Cu^{2+} did not shift the signal relative to that for Cu^{2+} only, implying coordination of Cu^{2+} with **2** suggesting weak binding. Interestingly, the EPR spectrum after 40 min incubation of **2** with Cu^{+}/Al^{3+} was silent, suggesting Cu^{+}·**2** binding did not allow for disproportionation to paramagnetic Cu^{2+}; or perhaps a minute amount of Cu^{+} was changed into Cu^{2+}, an amount below detection by EPR spectroscopy.

Binding sites of **2** with metal ions and H^{+} were examined using ^{1}H NMR analysis (Figure 3, ESI, Figure S13–S14). For the Cu^{+}-only case, a strong broadening effect on the urea NH (H_3) and imine protons (H_5), aromatic protons ($H_{7–10}$) and carbamoyl methyl protons ($H_{16–17}$) was shown, implying that Cu^{+} changed into Cu^{0} and Cu^{2+} to give a strong paramagnetic effect on the protons of the overall ligand (Figure 3). However, Cu^{+} with Al^{3+} showed a different ^{1}H NMR spectral pattern from the case of Cu^{+} only, *not total broadening* of ^{1}H NMR peaks. Comp. **2** with Al^{3+} and Cu^{+} exhibited *partial broadening* of the urea NH, imine hydrogen and aromatic hydrogens, excluding those for the carbamoyl group. In particular, the signal from the imine hydrogen signal (H_5) was too broad to be observed clearly indicated by the red arrow (Figure 3). This implies that the preference of Cu^{+} is to partially, but strongly, interact with the specific area (urea, imine, and aromatic region) of the ligand, distal to the carbamoyl group, and the binding mode of Cu^{+} with Al^{3+} is markedly different from that for Cu^{+} only.

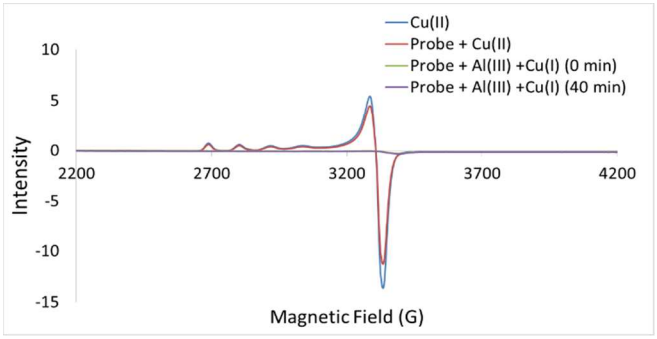

Figure 2. EPR spectral analysis of **2** with Cu^{+}, Cu^{2+} and Al^{3+}. Concentrations: Cu^{2+} (400 μM), **2** (200 μM) + Cu^{2+} (400 μM), **2** (200 μM) + Al^{3+} (200 μM) + Cu^{+} (200 μM), Solvent; acetonitrile mixed with 2 % (v/v) DMSO.

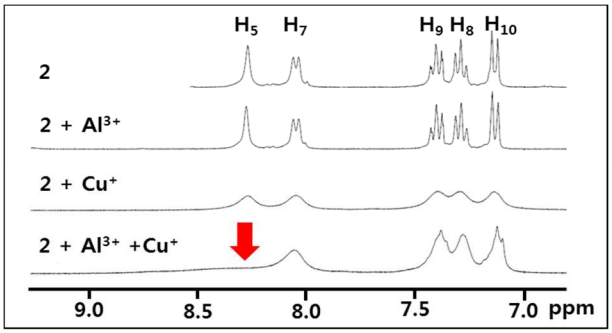

Figure 3. ^{1}H NMR analysis of **2** (1 equiv) with Al^{3+} (1 equiv), Cu^{+} (1 equiv), or Al^{3+} (1 equiv) + Cu^{+} (1 equiv) for verifying interaction sites at 9.2 ppm – 6.9 ppm. Solvent: DMSO–d_6 + D_2O (4.3 v/v %).

Fluorescence mechanism in this probing system elicits three points of discussion. (*i*) Cu^{+} fluorescence signal in the presence of Al^{3+} showed the same emission wavelength as that for Cu^{2+} (Figure 1). (*ii*) H^{+} generated by Al^{3+} in aqueous solution contributed greatly to Cu^{+} fluorescence (ESI, Figure S11). (*iii*) Although **2** does not possess soft donor atoms ideal for binding Cu^{+}, Cu^{+} binding with **2** in the presence of Al^{3+} was bound strong and stable enough so that Cu^{+} cannot be substituted with Cu^{2+} or Al^{3+} or disproportionation as seen through the interference, titration experiments, and EPR analysis (Figure 1-2, ESI, Figure S5, S10).

To rationalize these phenomena, a *redox non–innocence mechanism* can be proposed (ESI, Figure S20). Redox non–innocence has been reported in many studies,[21-25] and deals with stabilizing the coordination between transition metal ions and ligands and electron transfer between the transition metal ions and the ligand without a spin multiplicity change, which induces higher or lower oxidation states of the transition metal ion to induce a more stable interaction. Through the UV–visible absorbance results for **2** with Cu^{+} and Al^{3+}, a new long wavelength peak at 460 nm (ESI, Figure S8(c)) was revealed, evident of a redox non–innocent system.[26, 27] This redox non–innocence allows us to explain three previous points of discussion. Cu^{+} gives one electron to the ligand and changes into Cu^{2+} without a spin multiplicity change based on EPR spectroscopic results. Cu^{2+}, in a higher oxidation state than Cu^{+}, can bind strongly with the ligand; although this probe has no softer elements like sulfur, from interference results and titration results (ESI, Figure S5, S10), this shows the same emission maximum wavelength, similar to the result for Cu^{2+} alone. For electron transfer, a positive species like H^{+} appears to take on an important role to decrease the activation energy of electron (negative charge) transfer from Cu^{+} to the ligand.[28] Consequently, the transferred single electron is distributed around the entire ligand except for the carbamoyl group, which explains the partial broadening effect on ^{1}H-NMR signal at urea NH, imine hydrogen and aromatic hydrogens. In particular, for H^{+} binding in the ligand, the imine nitrogen (N_4) is the most adequate because of its strong basicity. Therefore, an electron transferred from Cu^{+} can remain for a relatively long time in the protonated imine area, which induces a strongly broadening effect observed in the ^{1}H-NMR signal of the imine proton (H_5) in Figure 3 (red arrow).

Electrochemical experiments are performed to clarify oxidation state of copper in metal complex (Figure 4). The blue line represents electrochemical properties of 2 mM Cu^{+} in 0.1 M TBAP in DMSO. Cu^{+} shows cathodic (E_{pc}) and anodic (E_{pa}) peak potentials at -0.65 and -0.57 V vs Fc^{+}/Fc, respectively ($E^{0'}$ = -0.62 V vs Fc^{+}/Fc, approximately). However, when copper(I) was present with the protonated ligand, additional redox peaks appeared (red line), strongly suggesting metal ligand complexation, E_{pa1}, E_{pc1}, E_{pa2}, and E_{pc2} at -0.03, -0.30, -0.35 and -0.50 V vs Fc^{+}/Fc, respectively. This reveals that there are two redox reaction steps in the metal complex: $E_1^{0'}$ = -0.17 V vs Fc^{+}/Fc and $E_2^{0'}$ = -0.43 V vs Fc^{+}/Fc for each step. Although Figure S21 shows that ligand is not electroactive, when Cu^{+} is combined with protonated ligand, Cu^{+} donates one electron to the ligand and changes oxidation state from copper(I) to copper(II). As a result, we conclude that there exist "redox non-innocent" characteristics of the ligand that affect the oxidation state of the metal.

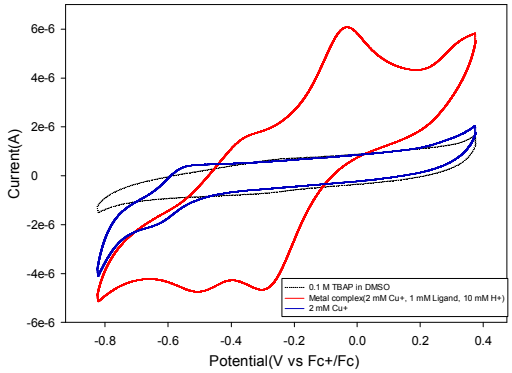

Figure 4. Cyclic voltammetry of Comp. **2** with Cu^{+} and H^{+}.

As shown in Scheme 3 and in the ESI. (Figure S9-10) Crucial fluorescence signal changes were observed under various conditions of Comp. **2**, Cu^{2+}, Al^{3+}, Cu^{+}, and L-cysteine. From the result for Comp. **2**, with Cu^{2+} and L-cysteine, were able to allow for the construction of an 'INH' molecular logic gate (Scheme 3 (*left*)). In addition, as shown in Figure S10, the two output signals at 345 nm and 445 nm were observed in the presence of Al^{3+}, Cu^{+}, and Comp. **2**, which were arranged to signify a 1:2 DEMULTIPLEXING' logic gate (Scheme 3 (*right*)).[29]

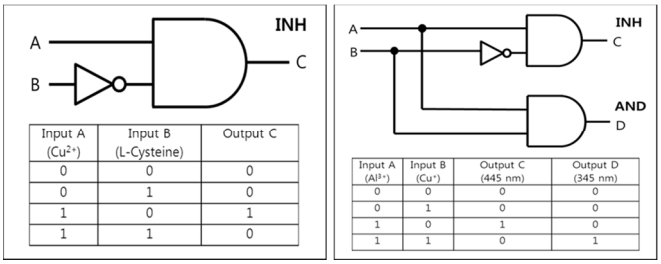

Scheme 3. Construction of molecular logic gates for Cu^{2+}, Al^{3+}, Cu^{+} and L-cysteine. (*left*) 'INH' logic gate for Cu^{2+} and L-cysteine, (*right*) '1:2 DEMULTIPLEXING' logic gate from Al^{3+} and Cu^{+}.

Prof. David G. Churchill (D. G. C.) acknowledges support from the NRF (National Research Foundation) of Korea (2011–0017280, NRF-2014R1A2A1A11052980), and the End-Run Project of KAIST (N01140684). Sudesh T. Manjare acknowledges the support from Institute of Basic Science (IBS). EPR analysis were performed through the support of the Korea Basic Science Institute (KBSI, Daejeon). Prof. Yoon Sup Lee acknowledges NRF grant # (2007–0056095) and computational resources from KISTI (KSC–2012–C2–41). YH acknowledges comments from Prof. Dongwhan, Lee at Dept. of Chemistry, Seoul National University, and Prof. Mu–Hyun, Baik at Dept. of Chemistry, Indiana University.

Notes and references

[a] Department of Chemistry, Korea Advanced Institute of Science and Technology (KAIST), 373–1 Guseong–dong, Yuseong–gu, Daejeon, 305–701, Republic of Korea.

[b] Center for Catalytic Hydrocarbon Functionalizations, Institute for Basic Science (IBS), 373−1 Guseong−dong, Yuseong−gu, Daejeon, 305−701, Republic of Korea.

† The present affiliations of DPM (postdoctoral fellow) and STM (assistant professor) are Korea Institute of Science and Technology (KIST), Seoul, Republic of Korea, and Dept. of Chemistry, University of Mumbai, India, respectively.

† Synthesis of the probe, NMR data (^{1}H, ^{13}C), DFT results, Job plotting results, titration results, reversibility data by biothiols, and experiments about the probing reliability of Cu^{+} in this system can be seen in electronic supporting information (ESI): See DOI: 10.1039/c000000x/

1. C. J. Fahrni, *Curr. Opin. Chem. Biol.*, 2013, **17**, 656-662.
2. M. T. Morgan, P. Bagchi and C. J. Fahrni, *J. Am. Chem. Soc.*, 2011, **133**, 15906-15909.
3. X. W. Cao, W. Y. Lin and W. Wan, *Chem. Commun.*, 2012, **48**, 6247-6249.
4. M. Taki, S. Iyoshi, A. Ojida, I. Hamachi and Y. Yamamoto, *J. Am. Chem. Soc.*, 2010, **132**, 5938-+.
5. A. F. Chaudhry, S. Mandal, K. I. Hardcastle and C. J. Fahrni, *Chem. Sci.*, 2011, **2**, 1016-1024.

6. Y. Zhou, F. Wang, Y. Kim, S. J. Kim and J. Yoon, *Org. Lett.*, 2009, **11**, 4442-4445.
7. O. Garcia-Beltran, N. Mena, L. C. Friedrich, J. C. Netto-Ferreira, V. Vargas, F. H. Quina, M. T. Nunez and B. K. Cassels, *Tetrahedron Lett.*, 2012, **53**, 5280-5283.
8. H. C. Lan, B. Liu, G. L. Lv, Z. H. Li, X. D. Yu, K. Y. Liu, X. H. Cao, H. Yang, S. P. Yang and T. Yi, *Sens. Actuators, B*, 2013, **173**, 811-816.
9. J. X. Yin, X. Ma, G. H. Wei, D. B. Wei and Y. G. Du, *Sens. Actuators, B*, 2013, **177**, 213-217.
10. S. Khatua, S. H. Choi, J. Lee, J. O. Huh, Y. Do and D. G. Churchill, *Inorg. Chem.*, 2009, **48**, 1799-+.
11. K. P. Kepp, *Chem. Rev.*, 2012, **112**, 5193-5239.
12. W. H. Ding, C. Wei, X. J. Zheng, D. C. Fang, W. T. Wong and L. P. Jin, *Inorg. Chem.*, 2013, **52**, 7320-7322.
13. Y. G. Zhao, Z. H. Lin, H. P. Liao, C. Y. Duan and Q. J. Meng, *Inorg. Chem. Commun.*, 2006, **9**, 966-968.
14. M. Arduini, F. Felluga, F. Mancin, P. Rossi, P. Tecilla, U. Tonellato and N. Valentinuzzib, *Chem. Commun.*, 2003, 1606-1607.
15. H. M. Park, B. N. Oh, J. H. Kim, W. Qiong, I. H. Hwang, K. D. Jung, C. Kim and J. Kim, *Tetrahedron Lett.*, 2011, **52**, 5581-5584.
16. L. Zeng, E. W. Miller, A. Pralle, E. Y. Isacoff and C. J. Chang, *J. Am. Chem. Soc.*, 2005, **128**, 10-11.
17. M. T. Morgan, P. Bagchi and C. J. Fahrni, *Dalton Trans.*, 2013, **42**, 3240-3248.
18. A. Velavan, S. Sumathi and K. K. Balasubramanian, *Eur. J. Org. Chem.*, 2013, 3148-3157.
19. A. Ohkubo, R. Kasuya, K. Miyata, H. Tsunoda, K. Seio and M. Sekine, *Org. Biomol. Chem.*, 2009, **7**, 687-694.
20. Y. Ha, A. Yang, S. Lee, K. Kim, H. Liew, S. H. Lee, J. E. Lee, H. I. Lee, Y. H. Suh, H. S. Park and D. G. Churchill, *J. Neurosci. Res.*, 2014, **92**, 359-368.
21. V. Lyaskovskyy and B. de Bruin, *ACS Catalysis*, 2012, **2**, 270-279.
22. I. S. Ke, J. S. Jones and F. P. Gabbai, *Angew. Chem. Int. Ed.*, 2014, **53**, 2633-2637.
23. A. F. Cozzolino, C. K. Brozek, R. D. Palmer, J. Yano, M. Y. Li and M. Dinca, *J. Am. Chem. Soc.*, 2014, **136**, 3334-3337.
24. F. Heims, F. F. Pfaff, S. L. Abram, E. R. Farquhar, M. Bruschi, C. Greco and K. Ray, *J. Am. Chem. Soc.*, 2014, **136**, 582-585.
25. Y. Dede, X. H. Zhang, M. Schlangen, H. Schwarz and M. H. Baik, *J. Am. Chem. Soc.*, 2009, **131**, 12634-12642.
26. W. M. Khairul, M. A. Fox, P. A. Schauer, D. Albesa-Jove, D. S. Yufit, J. A. K. Howard and P. J. Low, *Inorg. Chim. Acta*, 2011, **374**, 461-471.
27. L. Y. Tian, Y. M. Liu, G. X. Tian, X. H. Wu, Z. Li, J. F. Kou, Y. P. Ou, S. H. Liu and W. F. Fu, *Dalton Trans.*, 2014, **43**, 4093-4101.
28. P. B. Chatterjee, O. Goncharov-Zapata, G. J. Hou, O. Dmitrenko, T. Polenova and D. C. Crans, *Eur. J. Inorg. Chem.*, 2012, 4644-4651.
29. A. P. de Silva, *Chem. Asian J.*, 2011, **6**, 750-766.

